KeAi
CHINESE ROOTS
GLOBAL IMPACT

International Journal of Innovation Studies

ONLINE DIAGNOSIS OF WINDING AXIAL DISPLACEMENT IN POWER TRANSFORMERS BASED ON REAL-TIME CHANGES IN SHORT-CIRCUIT IMPEDANCE

Milad Bandehzadeh
PhD Candidate, Department of Engineering, Islamic Azad University Central Tehran Branch, Tehran, Iran (email: milad_bandehzadeh@yahoo.com)

Hamid Radmanesh
Corresponding Author : Department of Engineering, Islamic Azad University Central Tehran Branch, Tehran, Iran (email: h.radmanesh@iauctb.ac.ir)

Payam Rabbanifar
Department of Engineering, Islamic Azad University Central Tehran Branch, Tehran, Iran (email: pay.rabanifar@iauctb.ac.ir

Shahram Javadi
Department of Engineering, Islamic Azad University Central Tehran Branch, Tehran, Iran (email: sh.javadi@iauctb.ac.ir)

Abstract—Power transformers represent critical assets within electrical power systems, and the implementation of online fault diagnosis has garnered considerable research interest in recent years. Short-circuit impedance stands out as a fundamental parameter significantly influencing transformer design. Under the intense electromagnetic forces arising during short-circuit events, transformer windings are susceptible to deformation, with axial displacement being a prominent type of damage. Such axial displacement can induce measurable alterations in the transformer's short-circuit impedance. This paper presents an investigation into the online diagnosis of winding axial displacement in power transformers by analyzing real-time changes in short-circuit impedance. Utilizing finite element method (FEM) simulations, the study compares various components of the leakage flux density, the net leakage flux density, percentage reactance, and percentage impedance. The sensitivity and monotonic behavior of these parameters with respect to axial displacement in both the low-voltage and high-voltage windings are thoroughly evaluated.

Key Words—Power Transformer, Winding Axial Displacement, Online Diagnosis, Transfer Function, Short Circuit Impedance.

I. INTRODUCTION

The short-circuit impedance of a transformer is a critical parameter significantly influencing its overall design [1]. During short-circuit faults, the substantial electromagnetic forces generated can lead to the deformation of power transformer windings [2]-[7], with axial displacement being a common consequence of these forces [1]-[2], [7]. The winding structure dictates the distribution and magnitude of the leakage magnetic field within the transformer

[8]-[9], and any axial displacement of the windings can consequently alter the short-circuit impedance. Therefore, monitoring the short-circuit impedance and comparing measured values against historical data or factory test results presents an effective methodology for diagnosing winding deformation [1], [8]. This approach essentially relies on the analysis of impedance changes over time. The percentage impedance, a value specified by transformer users, typically ranges from a low of 2% for smaller distribution transformers to as high as 20% for large power transformers. Impedance values outside this range are reserved for specialized applications [1], [5]. Given this typical impedance range, potential short-circuit currents in power transformers can vary from 5 to 50 times the rated current. Consequently, the resulting short-circuit forces can escalate to 25 to 2500 times the forces experienced under rated current conditions. This highlights the crucial impact of the impedance percentage on the mechanical stability of transformers. Various techniques exist for calculating inductance in transformers, including the energy-based method, finite element method (FEM), method of images, Roth's method, and Rabin's method [1]-[8]. While three-dimensional (3D) FEM offers high accuracy, it may not always be necessary given the typical tolerance range for impedance values, which is often ±7.5% or ±10% [1], [11]. Consequently, two-dimensional (2D) FEM simulations have been extensively utilized in prior research for transformer inductance calculations, yielding acceptable agreement with analytical methods, 3D FEM simulations, and experimental measurements [9]-[10], [12]-[13]. A significant portion of the leakage flux surrounding transformer windings is oriented axially. The axial leakage flux reaches its maximum intensity around the mid-height of the windings when no axial displacement exists between the low-voltage and high-voltage windings. In the absence of axial displacement, radial leakage fluxes are considerably weaker than their axial counterparts, reaching their peak values at the top and bottom of the windings. However, relative axial displacement between the windings disrupts this flux distribution, altering both the radial and axial leakage fluxes. These changes are attributed to the development of an unbalanced magneto-motive force (MMF) [1]-[2], [5], [14], ultimately leading to a change in the transformer's impedance percentage.

This paper investigates the online diagnosis of winding axial displacement in power transformers through the real-time calculation of short-circuit impedance. The sensitivity of this diagnostic method to varying levels of axial displacement is quantified.

II. HEALTHY TRANSFORMER FEM SIMULATION

The key specifications of the single-phase transformer under investigation are detailed in Table 1. Notably, the high-voltage (HV) winding features a disk-type construction, while the low-voltage (LV) winding is of the layer type.

TABLE. 1. SPECIFICATION OF THE TRANSFORMER [7]

Parameter	Definition	Value	Unit
S_{rated}	Rated Apparent Power	1.6	MVA
$V_{rated,HV}$	Rated Voltage of High Voltage (HV) Winding	20	kV
$V_{rated,LV}$	Rated Voltage of Low Voltage (LV) Winding	0.4	kV
U_k	Impedance Percent	5.85	%

f_{rated}	Rated Frequency	50	Hz
$N_{Disks,HV}$	Number of Disks in HV Winding	38	-
$N_{T,\ End\ Disks}$	Number of Turns in 8 Bottom and 8 Top Disks of HV Winding	20	-
$N_{T,\ Intermediate\ Disks}$	Number of Turns in 22 Intermediate Disks of HV Winding	21	-
$N_{Layers,LV}$	Number of Layers in LV Winding	2	-
$N_{T,Layers,LV}$	Number of Turns in each Layer of LV Winding	13	-
$N_{Paral.\ Cond.,\ LV}$	Number of Paralleled Conductors in LV Winding	3	-
$R_{in,\ LV}$	Internal Radius of the LV winding	93	mm
$R_{out,\ LV}$	External Radius of the LV winding	106	mm
$D_{LV,\ Layers}$	Distance between the Layers of the LV winding	4	mm
$D_{LV,\ HV}$	Distance between the LV and HV windings	12.5	mm
$R_{in,\ HV}$	Internal Radius of the HV winding	118.5	mm
$R_{out,\ HV}$	External Radius of the HV winding	176.5	mm
Cond. $_{LV,Dim}$	Dimensions of the LV Conductors	3.35 * 11.8	mm^2
Cond. $_{HV,Dim}$	Dimensions of the HV Conductors	2.12 * 8.5	mm^2
W_{ins}	Thickness of the Insulation Paper	0.5	mm
H_{LV}	Height of the LV winding	536	mm
H_{HV}	Height of the HV winding	494	mm
R_{core}	Core Radius	90	mm

A two-dimensional (2D) Finite Element Method (FEM) simulation was conducted using COMSOL Multiphysics software. The simulation employed the H-formulation as its governing equation, directly solving for the magnetic field components derived from Ampere's and Faraday's laws as (1).

$$\partial(\mu H)/\partial t + \text{curl}(\rho\ \text{curl}(H))=0 \quad (1)$$

Where H [A/m] is the magnetic field intensity, μ [H/m] is the magnetic permeability and ρ [Ω.m] is the electrical resistivity.

The computational resources utilized for these simulations included a system with 64 processor cores and 128 GB of RAM. The resulting magnetic flux density distribution within the studied transformer under rated load conditions is illustrated in Fig. 1. Further visualization of the magnetic flux density is provided through arrow surfaces and arrow lines in Fig. 2, and Fig. 3.

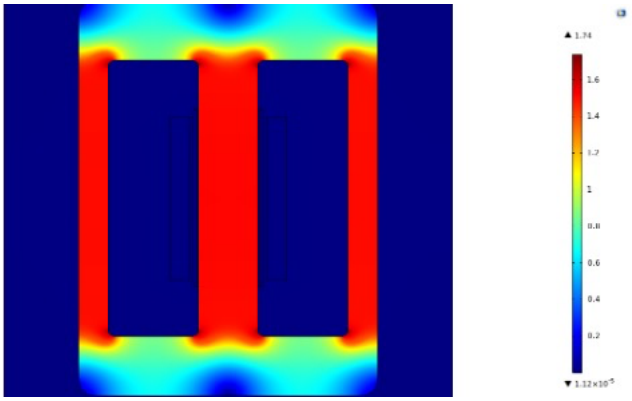

Fig. 1. Distribution of magnetic flux density in the studied transformer.

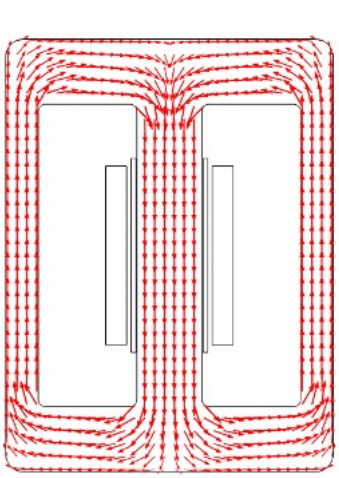

Fig. 2. Arrow surface of magnetic flux density in the studied transformer.

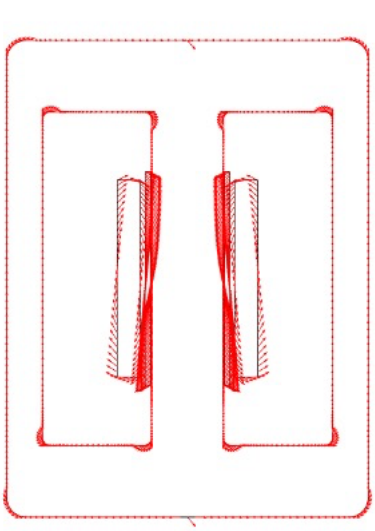

Fig. 3. Arrow line of magnetic flux density in the studied transformer.

Using energy-based method (magnetic stored energy), inductance of the transformer has been calculated from the outputs of the FEM simulation as (2)-(3).

$$L = 2W/I^2 \quad (2)$$

$$L = 1/I^2 \int_v B.H\, dv = 1/I^2 \int_v A.J\, dv \quad (3)$$

Where, W [J] is the magnetic energy, I [A] is the current, L [H] is the inductance, B [T] is the magnetic flux density, A [Wb/m], and J [A/m2] is the current density.

Then reactance percent can be calculated by multiplying inductance (referred to LV side) to 2πfrated*Srated/V2rated,LV *100%. Also, by dividing Ohmic losses in rated load condition to Srated and then multiplying to 100%, series resistance percent can be calculated. As output of the simulation, ohmic losses in the rated load condition is equal to 19900 W, Therefor resistance percent is equal to 1.24 %. Reactance percent as the output of the FEM simulation is equal to 5.47%. Thus impedance percent as the output of the FEM simulation is equal to sqrt(5.472 + 1.242)=5.61 %. Thus, the output of the FEM simulation has shown (5.61-5.85)/5.85*100% = -4.1% error with respect to the transformer specification provided by the manufacture. This error value is acceptable and shows the high accuracy of the FEM simulation.

III. FEM SIMULATION OF TRANSFORMER WITH AXIALLY DISPLACED WINDINGS

Downward axial displacement was simulated for both the low-voltage (LV) and high-voltage (HV) windings. The displacement values considered in the simulations were 15 mm, 30 mm, 45 mm, and 60 mm for both windings. Due to page limit and just geometry and arrow line of magnetic flux density in the studied transformer with 60 mm downward axial displacement in the HV winding has been presented in Fig. 4. In this case we can see the asymmetry in the distribution of the arrow lines of the magnetic flux density. This asymmetry is not available in the Fig. 3, which not has axial displacement. In another words, we can see that in Fig. 3, at the mid height of the windings direction of the arrow lines are changed but in Fig. 4. The point of

the direction change in the windings is somewhere lower than the mid height of the windings. This changed distribution will change the magnitude of the axial and radial components of the magnetic flux density along the height of the windings and therefor will change the impedance percent.

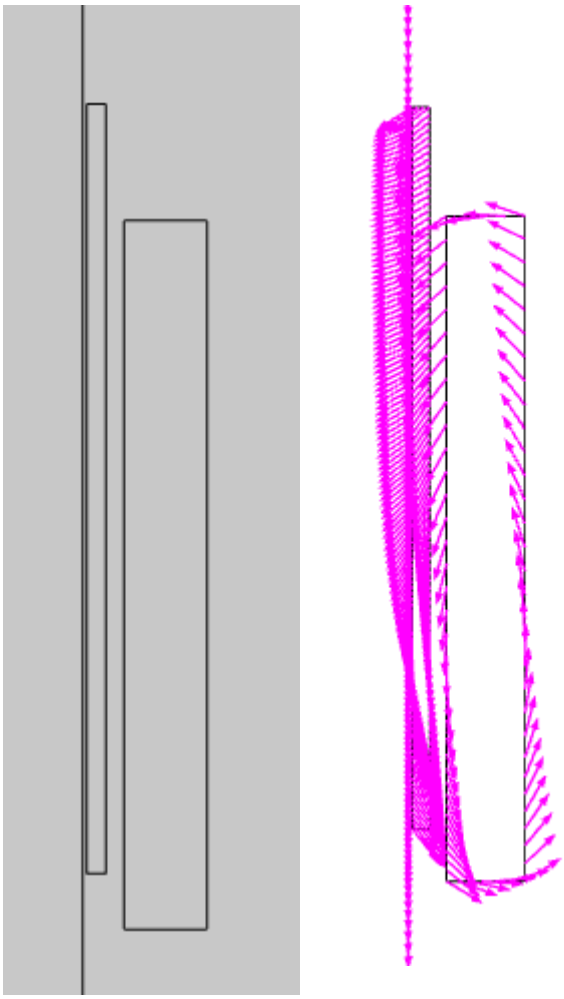

Fig. 4. Geometry and arrow line of magnetic flux density in the studied transformer with 60 mm downward axial displacement in the HV winding.

Different output parameters of the transformer have been extracted from the FEM simulations and presented in Tables 2 to 6.

TABLE. 2. REACTANCE PERCENT OF THE STUDIED TRANSFORMER

Displacement on	Downward Displacement Value (mm)	Reactance Percent (Ux %)	Change Percent versus Healthy Case
Healthy Case	-	5.47	-

LV Winding	15	5.94	8.65
	30	6.36	16.35
	45	6.78	24.04
	60	7.10	29.81
HV Winding	15	6.21	13.46
	30	6.94	26.92
	45	7.68	40.38
	60	8.42	53.85

The data presented in Table 2 indicates that the percentage change in reactance is more pronounced when axial displacement occurs in the high-voltage (HV) winding compared to an equivalent displacement in the low-voltage (LV) winding. Furthermore, Table 2 reveals a monotonic and incremental relationship between the percentage change in reactance and the magnitude of axial displacement for both cases (LV and HV winding displacement).

TABLE. 3. IMPEDANCE PERCENT OF THE STUDIED TRANSFORMER

Displacement on	Downward Displacement Value (mm)	Impedance Percent (Uk %)	Change Percent versus Healthy Case
Healthy Case	-	5.61	-
LV Winding	15	6.07	8.22
	30	6.48	15.58
	45	6.9	22.95
	60	7.21	28.48
HV Winding	15	6.33	12.82
	30	7.05	25.71
	45	7.78	38.65
	60	8.51	51.63

The data presented in Table 3 indicates that the percentage change in impedance is more pronounced when axial displacement occurs in the high-voltage (HV) winding compared to an equivalent displacement in the low-voltage (LV) winding. Furthermore, Table 3 reveals a monotonic and incremental relationship between the percentage change in impedance and the magnitude of axial displacement for both cases (LV and HV winding displacement).

TABLE. 4. MAXIMUM OF THE AXIAL COMPONENT OF LEAKAGE FLUX DENSITY ALONG THE HEIGHT OF THE WINDINGS OF THE STUDIED TRANSFORMER

Displacement on	Downward Displacement Value (mm)	Maximum of the Axial Component of Leakage	Change Percent versus Healthy Case

		Flux Density (T)	
Healthy Case	-	0.00327	-
LV Winding	15	0.0033	0.92
	30	0.00333	1.83
	45	0.00333	1.83
	60	0.0337	3.06
HV Winding	15	0.00333	1.83
	30	0.00333	1.83
	45	0.00335	2.45
	60	0.00337	3.06

The data presented in Table 4 indicates that the percentage change in the maximum axial component of the leakage flux density along the winding height is more pronounced when axial displacement occurs in the high-voltage (HV) winding compared to an equivalent displacement in the low-voltage (LV) winding. Furthermore, Table 4 reveals a non-monotonic yet incremental relationship between the percentage change of this parameter and the magnitude of axial displacement for both cases (LV and HV winding displacement).

TABLE. 5. MAXIMUM OF THE RADIAL COMPONENT OF LEAKAGE FLUX DENSITY ALONG THE HEIGHT OF THE WINDINGS OF THE STUDIED TRANSFORMER

Displacement on	Downward Displacement Value (mm)	Maximum of the Radial component of Leakage Flux Density (T)	Change Percent versus Healthy Case
Healthy Case	-	0.00389	-
LV Winding	15	0.00405	4.11
	30	0.00419	7.71
	45	0.00433	11.31
	60	0.00448	15.17
HV Winding	15	0.00418	7.46
	30	0.00446	14.65
	45	0.00473	21.59
	60	0.00501	28.79

The data presented in Table 5 indicates that the percentage change in the maximum radial component of the leakage flux density along the winding height is more pronounced when axial displacement occurs in the high-voltage (HV) winding compared to an equivalent displacement in the low-voltage (LV) winding. Furthermore, Table 5 reveals a monotonic and incremental

relationship between the percentage change of this parameter and the magnitude of axial displacement for both cases (LV and HV winding displacement).

TABLE. 6. MAXIMUM OF THE NET LEAKAGE FLUX DENSITY ALONG THE HEIGHT OF THE WINDINGS OF THE STUDIED TRANSFORMER

Displacement on	Downward Displacement Value (mm)	Maximum of the Net Leakage Flux Density (T)	Change Percent versus Healthy Case
Healthy Case	-	0.00475	-
LV Winding	15	0.00497	4.63
	30	0.00515	8.42
	45	0.00515	8.42
	60	0.00544	14.53
HV Winding	15	0.00508	6.95
	30	0.00564	18.74
	45	0.00564	18.74
	60	0.0059	24.21

The data presented in Table 5 indicates that the percentage change in the maximum radial component of the leakage flux density along the winding height is more pronounced when axial displacement occurs in the high-voltage (HV) winding compared to an equivalent displacement in the low-voltage (LV) winding. Furthermore, Table 5 reveals a non-monotonic yet generally increasing (incremental) relationship between the percentage change of this parameter and the magnitude of axial displacement for both cases (LV and HV winding displacement).

Among the abovementioned parameters, for detecting the real time changes in the reactance and impedance percents we should have online monitoring of the parameters (voltage, current, power factor, apparent power, active power and reactive power) at the both LV and HV sides of the transformer.

Also, for detection of the axial, radial and net components of the leakage flux density along the height of windings, we should install flux sensors in some different point along the height of the windings which are very much difficult than real time detection of reactance or impedance percents.

IV. CONCLUSION

This study has successfully investigated the feasibility of online diagnosis of winding axial displacement in power transformers by analyzing real-time changes in short-circuit impedance. Through comprehensive simulations utilizing the finite element method (FEM), various key parameters, including different components of the leakage flux density, net leakage flux density, percentage reactance, and percentage impedance, were meticulously compared under

conditions of axial winding displacement. The analysis of the simulation results unequivocally identifies the percentage reactance as the most sensitive indicator and the most effective parameter among those examined for detecting axial displacement. Notably, a substantial change of 53.85% in the percentage reactance was observed in comparison to the healthy (undisplaced) state. This significant alteration occurred under a 60 mm downward axial displacement of the high-voltage (HV) winding, highlighting the considerable impact of HV winding displacement on this parameter. Furthermore, the change in percentage reactance exhibited a desirable monotonic and incremental behavior with increasing displacement values for both the low-voltage (LV) and high-voltage (HV) windings, indicating a consistent and predictable relationship that can be effectively utilized for diagnostic purposes. This monotonic trend strengthens the reliability of using reactance percentage changes as a direct indicator of the extent of axial displacement. The significant sensitivity of the reactance percentage to axial displacement, particularly in the HV winding, suggests its potential as a robust parameter for developing online monitoring and diagnostic systems for power transformers. The monotonic and incremental nature of its change with increasing displacement further facilitates the establishment of a correlation between the measured reactance and the severity of the axial winding deformation. This finding underscores the practical applicability of monitoring real-time changes in short-circuit impedance, specifically the reactance component, as a proactive approach to detect and potentially mitigate the risks associated with axial winding displacement in power transformers, thereby contributing to enhanced operational reliability and reduced maintenance costs. Also, as discussed the cost and difficulty of real time detection of the reactance and impedance percents are much lower than the real time detection of radial, axial and net components of the leakage flux density.

Competing Interests

The authors wish to state that they have no known financial interests or personal relationships that could be perceived as having influenced the research presented in this paper.

REFERENCES

[1] S. V. Kulkarni and S. A. Khaparde, "Transformer Engineering Design, Technology and Diagnostics," Marcel Dekker, 2004.

[2] M. J. Heathcote, "The J&P Transformer Book," 13th ed., Elsevier, 2007.

[3] E. Rahimpour, J. Christian, K. Feser, and H. Mohseni, "Transfer function method to diagnose axial displacement and radial deformation of transformer windings," *IEEE Transactions on Power Delivery*, vol. 18, no. 2, pp. 493-505, Apr. 2003.

[4] A. Moradnouri, M. Vakilian, A. Hekmati, and M. Fardmanesh, "Optimal Design of Flux Diverter Using Genetic Algorithm for Axial Short-circuit Force Reduction in HTS Transformers," *IEEE Transactions on Applied Superconductivity*, vol. 30, no. 1, pp. 1-8, Jan. 2020.

[5] K. Karsai, D. Kerenyi, and L. Kiss, *Large Power Transformers*, Elsevier, 1987.

[6] W. M. Flanagan, "Handbook of Transformer Design & Applications," 2nd ed., McGraw-Hill, 1993.

[7] P. Karimifard, G. B. Gharehpetian, A. J. Ghanizadeh, and S. Tenbohlen, "Estimation of simulated transfer function to discriminate axial displacement and radial deformation of

transformer winding," *COMPEL: The International Journal for Computation and Mathematics in Electrical and Electronic Engineering*, vol. 31, no. 4, pp. 1277-1292, 2012.
[8] D. Allan and H. Moore, *Electric Power Transformer Engineering*, CRC Press, USA, 2004.
[9] Z. Ye *et al.*, "A Calculation Method to Adjust the Short-Circuit Impedance of a Transformer," *IEEE Access*, vol. 8, pp. 223848-223858, 2020, doi: 10.1109/ACCESS.2020.3042983.
[10] A. Moradnouri, M. Vakilian, A. Hekmati, *et al.*, "Inductance Calculation of HTS Transformers with Multi-segment Windings Considering Insulation Constraints," *J Supercond Nov Magn*, vol. 34, pp. 1329-1339, 2021.
[11] IEC 60076-5, *Power Transformers, Part 5: Ability to Withstand Short Circuit*, Edition 3, 2006.
[12] A. Ehsanifar, M. Dehghani, and M. Allahbakhshi, "Calculating the leakage inductance for transformer inter-turn fault detection using finite element method," in *2017 Iranian Conference on Electrical Engineering (ICEE)*, Tehran, Iran, 2017, pp. 1372-1377.
[13] M. Eslamian, M. Kharezy, and T. Thiringer, "An Accurate Analytical Method for Leakage Inductance Calculation of Shell-Type Transformers With Rectangular Windings," *IEEE Access*, vol. 9, pp. 72647-72660, 2021.
[14] A. MORADNOURI, M. VAKILIAN, P. ELHAMINIA, AND M. BAHRAMI, "INTRODUCTION OF DIMENSIONAL APPROACH TO EVALUATION OF DISTRIBUTION TRANSFORMER SHORT CIRCUIT FORCES," IN *2015 23RD IRANIAN CONFERENCE ON ELECTRICAL ENGINEERING*, TEHRAN, IRAN, 2015, PP. 1539-1544, DOI: 10.1109/IRANIANCEE.2015.7146464.